IEEE Access
Multidisciplinary | Rapid Review | Open Access Journal

Received 18 August 2023, accepted 2 September 2023, date of publication 7 September 2023,
date of current version 18 September 2023.

Digital Object Identifier 10.1109/ACCESS.2023.3312940

RESEARCH ARTICLE

Research on Path Planning for Robot Based on Improved Design of Non-Standard Environment Map With Ant Colony Algorithm

FENG LI[1,2], YOUNG-CHUL KIM[1], ZIANG LYU[1], AND HAN ZHANG[1]
[1]Department of Mechanical Engineering, Kunsan National University, Gunsan, Jeollabuk-do 54150, South Korea
[2]College of Smart Manufacturing, Zhengzhou University of Economics and Business, Zhengzhou 450007, China

Corresponding author: Young-Chul Kim (kimyc@kunsan.ac.kr)

This work was supported in part by the Science and Technology Research Project of Henan Province under Grant 222102210307 and Grant 182102210510.

ABSTRACT The maps used for the path planning of mobile robots are mostly grid maps, which are generated through independent design or sensor measurement to obtain relevant information and then modeling. To obtain the robot motion planning path more quickly, this paper proposes a method of robot motion path planning through the ant colony algorithm under a non-standard environment map. The non-standard environment map is used for standard grid design, and the grid map is optimized by the method of no safety distance added obstacle box selected and safety distance added obstacle box selected, then the path planning is carried out through the ant colony algorithm. In addition, the mutual correspondence between grid maps and real environment maps was solved by adding calibration objects. The experimental results show that this method can not only effectively solve the problem of ant colony algorithms under a non-standard real environment map, show the planning path and pose on the non-standard real environment map, moreover, the safety degree of the planning path in the real environment is also increased by 29.51%, ensuring the safety degree of the whole planning path, which improves the intelligent degree of robot motion path planning.

INDEX TERMS Robot path planning, non-standard map, grid map, ant colony algorithm, intelligence, safety degree.

I. INTRODUCTION

With the continuous progress and development of artificial intelligence technology, robots are now more and more applied to industry, agriculture, service industry, national defense, etc [1]. Now the factory uses industrial robots for welding and assembly is very common [2]. The use of robots in agriculture to spray pharmaceuticals and pick fruits is also very popular. Robots also exist in the service industry and military activities, either for transporting goods or for charging on the battlefield. Because robots can replace humans to engage in a variety of tasks today, the robot is increasingly becoming an indispensable auxiliary tool today [3], [4].

The associate editor coordinating the review of this manuscript and approving it for publication was Yang Tang.

As a high-tech product, the scope of research on robots is very broad. Now the popular research areas include special robots, robot path planning, and humanoid robots. In terms of special robots, to reduce personal accidents, mining robots are used in coal mines to replace human coal mining [5], and vascular intervention surgery robots can replace doctors to complete vascular internal intervention surgeries that cannot be completed by humans [6]. Construction robots can replace humans to brush walls and build houses, reducing labor intensity [7]. Fire robots can replace humans to rush into the sea of fire and extinguish fires [8]. Testing robots directly lead to the unemployment of quality testing workers [9]. In terms of robot path planning, various new intelligent algorithms have emerged one after another in recent years. In addition to the common ant colony algorithm and neural network algorithm, Ou et al. and others have conducted in-depth research on

This work is licensed under a Creative Commons Attribution-NonCommercial-NoDerivatives 4.0 License.
For more information, see https://creativecommons.org/licenses/by-nc-nd/4.0/

the gray wolf algorithm [10]. The foraging mechanism and group optimization algorithm studied the beetle group optimization algorithm [11], and Yang et al. studied the marine predator algorithm [12]. The research on the artificial fish swarm algorithm [13], the firefly algorithm [14], and the cuckoo search algorithm [15] are also relatively in-depth.

In recent years, there has also been a hot research topic on humanoid robots. The humanoid robot Atlas was developed by Boston Dynamics, the Fedor-850 humanoid robot developed by Russia, the CyberOne humanoid robot developed by China Xiaomi, and the ASIMO robot of Japan, all of which can replace human beings to complete certain work to a certain extent, and are highly intelligent. Both special robots and humanoid robots need to plan their motion paths, so robot motion path planning is very important. The map used in robot motion path planning is very important. The commonly used maps nowadays include occupancy grid maps, octo maps, and point cloud maps. Through research, it has been found that most of these robot motion maps are obtained by measuring the external environment through sensors, and then modeling and generating maps based on the measured information. In this way, establishing a map for robot motion path planning requires a lot of time, manpower, and material resources. The research group hopes to obtain non-standard maps of the real environment by taking photos of the environment that requires path planning. Then, perform relevant processing on this map so that it can be directly used for robot motion path planning. This not only saves a lot of time, but also saves manpower, material resources, and financial resources, which will bring about great progress.

In this study, the non-standard real environment map is processed, optimized, and improved to generate a grid map. The path planning is realized in the grid map through the ant colony algorithm, and the robot path planning under the non-standard environment map is realized by integrating the planning path with the non-standard map. The method proposed in this study converts the real environment map into a grid map. In order to make the grid map more standardized, some areas in the grid map have been improved, and the robot has been given ant colony algorithm path planning, and then the planning path is fed back to the real environment map, achieving the integration of the planning path and the real environment. To improve the safety of the planning path, the grid map is optimized by the method of no safety distance added obstacle box selected and safety distance added obstacle box selected, greatly improving the intelligent degree of the robot path planning. The expression is intuitive and the expression effect is good, so the research method in this article has broad application prospects.

The rest of this article is described as follows: the second part describes the research background of the topic and introduces the main path map planning methods and path map forming methods. The third part describes the preliminary research process. The fourth part discusses the problems encountered. The fifth part introduces the process of optimizing non-standard maps to generate standard grid maps, using a virtual reality environment, and then carries out the ant colony algorithm. The sixth part conducted experimental research and analysis through real environmental maps. The original, no safety distance added obstacle box selected and safety distance added obstacle box selected GM planning path is compared and analyzed in this part. The final section provides a summary of this article.

II. RESEARCH BACKGROUND

The planning of a robot's motion path is a complex process. On one hand, it requires a good expression of the robot motion environment map, and on the other hand, it requires the intelligent operation of the robot motion path planning algorithm, both of which are indispensable. The commonly used maps now include the Occupancy Grid Map, Octo Map, and Point Cloud Map. Konolige et al. developed the MURIEL method for updating occupied grids, which improved the fidelity of grid production [16]. Yuan et al. combined intelligent control methods to apply the Octo Map to drone control, achieving good results [17]. Choe et al. proposed a new method for mobile robot systems to reduce the size of 3D point cloud maps [18]. There are many common robot motion path planning methods, such as Ant colony algorithms(ACO), Dijkstra algorithm, A * algorithm, Random road map (PRM) algorithm, Rapidly expanding random tree (RRT) algorithm, Genetic algorithm (GA), etc. These algorithms are generally highly intelligent. Among these algorithms, the ant colony algorithms use a positive feedback mechanism, and the search keeps converging during the operation of the algorithm. In addition, it uses a heuristic probabilistic search method, which makes this algorithm not easy to fall into the local optimum, making it easier to find the global optimal solution, so it is widely used. By combining algorithms and maps, we can effectively plan the robot's motion path.

III. EARLY RESEARCH WORK

The mobile map of the robot plays an important role in the process of robot motion planning. But now, robot motion maps are mostly based on sensors measuring the environment to obtain relevant parameters, and then modeling based on the measured information. It is only implemented on the standard black and white grid map, and not implemented on the non-standard real environment map, like Table 1 [16], [17], [18], [19], [20], [21], [22], [23], [24], [25], [26], [27], [28], [29], [30], [31], [32], [33], [34], [35], [36], [37], [38]. This leads to the process requiring a lot of time, manpower, and material resources. In addition, how to ensure that the planning path does not conflict with obstacles and the robot does not contact with obstacles due to its own structure is only implemented through algorithms or methods to improve the accuracy of sensors. If a method can be found to quickly establish a robot's movement map in a non-standard real environment, and ensure the safety of the planning path, it will greatly reduce the difficulty of robot motion path planning. The research group hopes to directly use the non-standard real environment map for robot motion path planning after

TABLE 1. Comparison of different path planning methods using maps now.

Algorithm	The main map used	Measurement of dimensions using infrared or ultrasonic sensors, or free modeling	Safety guarantee method	Real environment map used
ACO	Grid map，Oto Map	Yes	Algorithm optimization improves the precision of sensor	No
A*	Grid map	Yes	Algorithm optimization improves the precision of sensor	No
PRM	Grid map	Yes	Algorithm optimization	No
PRT	Grid map	Yes	Algorithm optimization	No
RRT	Grid map， Octo Map	Yes	Algorithm optimization	No
GA	Grid map，	Yes	Algorithm optimization	No
PSO	Grid map， Point cloud map	Yes	Algorithm optimization	No

relevant processing and optimization. This not only saves a lot of time, but also saves manpower, material resources, and financial resources.

A. ESTABLISHMENT OF MAPS

The mobile map of a robot can effectively help the robot search for its motion path, and help the robot perceive and utilize the surrounding environment. The current common method for modeling robot mobile maps is to represent the robot's workspace as a large number of grids with binary information. If these grids contain obstacles, they are filled and represented in black. The absence of obstacles indicates that the robot can freely pass through, represented by white. White grids are generally represented by 0, while black grids are generally represented by 1, as Figure 1. The path planning of the robot becomes the optimization problem of connecting any two white grids in the map [39].

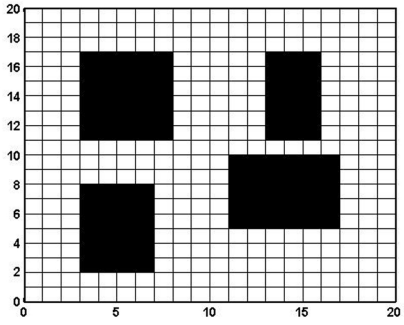

FIGURE 1. Standard grid map.

Based on the in-depth research on robot mobile maps, the research group obtained grid maps that can be used for robot path planning by binarizing, meshing, and filling the captured real environment map, as shown in Figure 1. This grid map is called a standard grid map because it is composed of black and white grids. The original captured real environment map is called a non-standard real environment map due to its color and irregular internal shape.

B. IMPLEMENTATION OF THE METHOD

After obtaining a standard grid map, we need to implement path planning for robots through the ant colony algorithm.

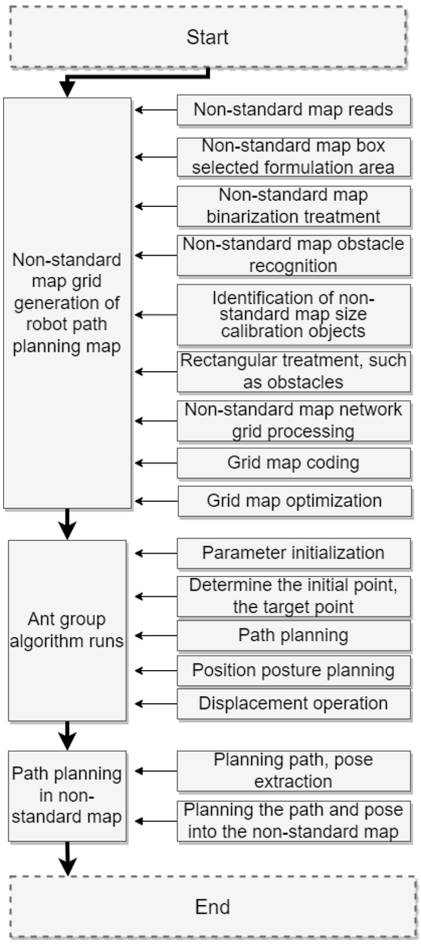

FIGURE 2. Non-standard map optimization robot path planning process.

Because of its strong robustness and good searchability, the ant colony algorithm has a wide range of applications. In order to better achieve path planning for mobile robots in non-standard environments, the research group first established a virtual non-standard environment for theoretical method testing [40].

C. THE OVERALL PROCESS

After getting the planning path of the mobile robot through ant colony algorithms, we return the planning path to the

FIGURE 3. Virtual non-standard map.

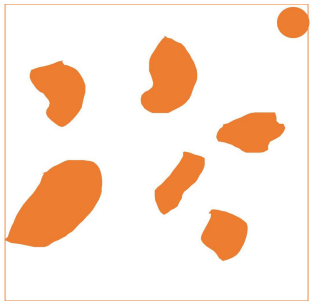

FIGURE 4. Virtual non-standard map box selected.

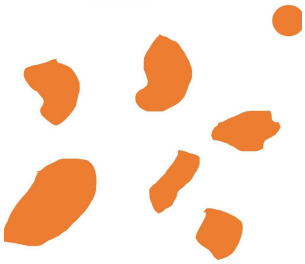

FIGURE 5. The cutting of the virtual nonstandard map.

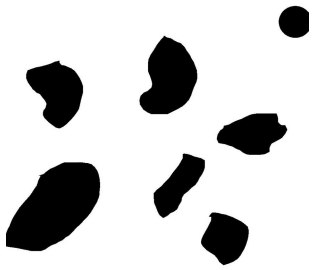

FIGURE 6. Virtual non-standard map binarization.

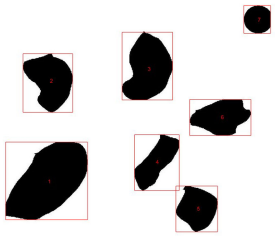

FIGURE 7. Virtual non-standard map obstacle recognition.

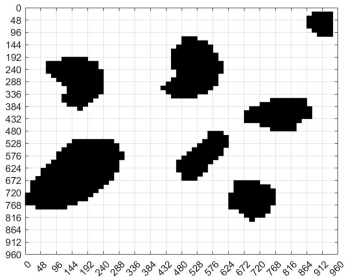

FIGURE 8. Virtual non-standard map GM map generation.

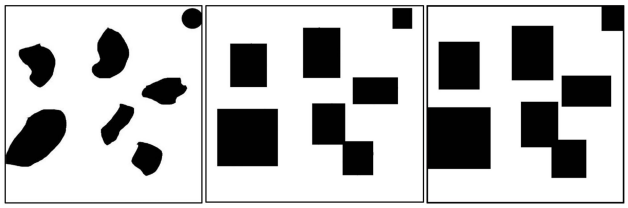

FIGURE 9. The maps of three methods. (a) Original unoptimized. (b) No safety distance added obstacle box selected. (c) Safety distance added obstacle box selected.

original non-standard real environment map. The planning path, planning position, and pose of the ant colony algorithm in the grid map standard environment are displayed on the non-standard real environment map, and the path planning of the mobile robot in the non-standard real environment is finally completed. In addition, by adding a calibration object to the map, the generated non-standard map can truly reflect the planning path of the robot, so the research significance of this method is enormous.

IV. DESCRIPTION OF THE PROBLEM

Through the above introduction, it is understood that when converting non-standard environmental maps into standard grid maps for robot path planning, it is necessary to binarize non-standard maps through the binarization method. In the process of researching path planning for non-standard maps of robots, we found that when performing grid processing after binary conversion on non-standard maps, there may be some phenomena of missing or increasing black grids in obstacle areas due to grid size. In addition, due to the structural problems of the robot itself, the planning path may also lead to contact between the robot and the obstacles during the moving process. To address these issues and improve the standardization level of non-standardized map grid processing, we conducted more in-depth research [41], [42].

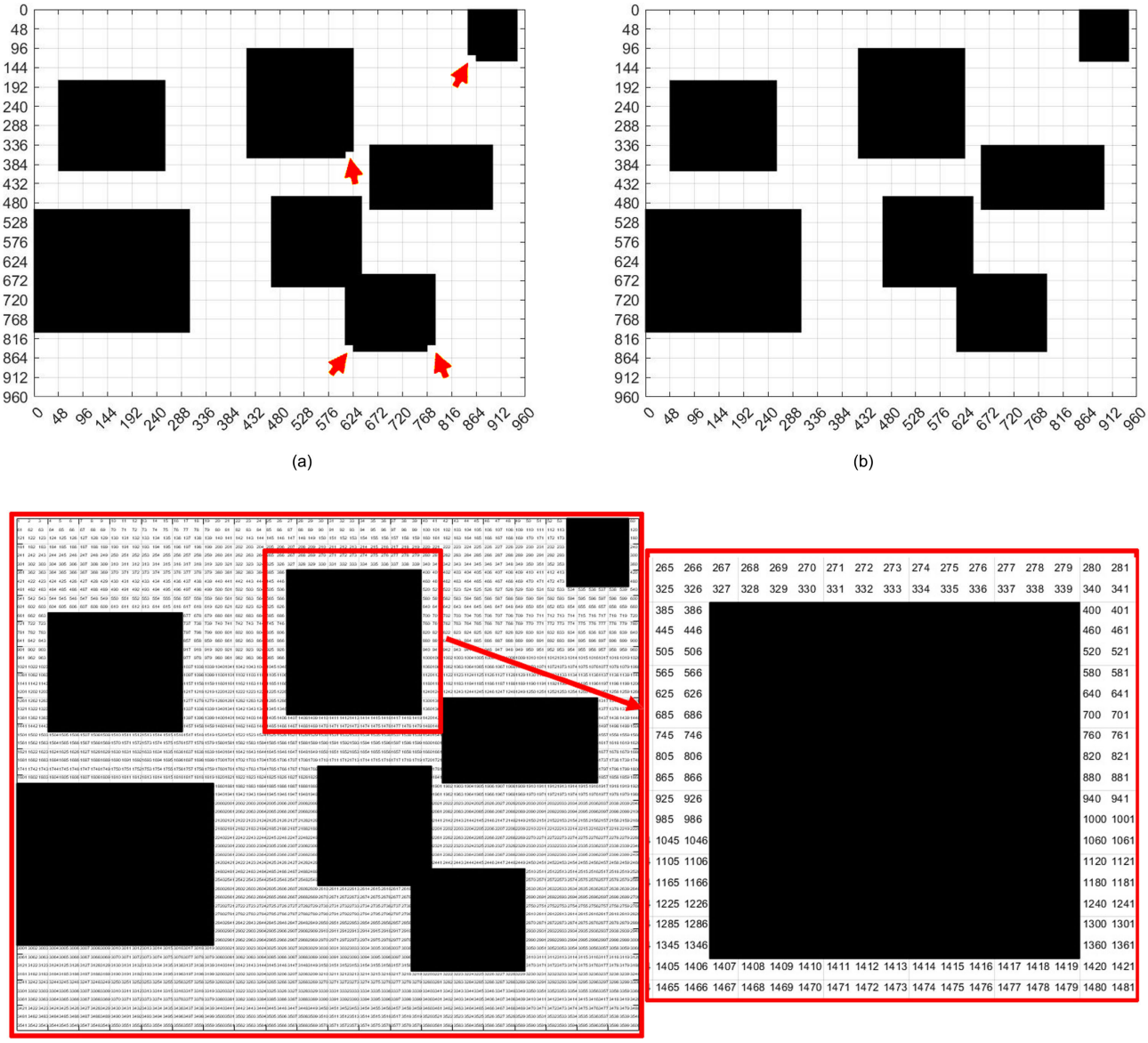

FIGURE 10. Virtual non-standard map grid design and encoding. (a) The GM map in the optimization process of non-standard map. (b) The GM map after the optimization of the non-standard map. (c) Grid Map Encoding.

V. METHOD

A. OVERALL FRAMEWORK

According to the above introduction, combined with the ant colony algorithm, we designed the robot path planning process under the non-standard environment map. This process is an improvement in the research method of the early stage. It incorporates improved processing of non-standard map gridding. This improves the mobile environment of robots, makes the entire grid map more standard, and makes it easy to implement the ant colony algorithm, as shown in Figure 2.

The planning process in Figure 2 mainly includes five major steps. First, open the Matlab software to enter the platform interface. We set the root directory for processing in the folder of the non-standard map to be planned and then perform grid processing on the non-standard map to convert it into a standard grid map. In this process, grid region selection, cropping, binarization processing, obstacle, and calibration target recognition are needed.

To optimize the map, make the generated grid map more standardized, and ensure the safety of the final planning path, it is also necessary to perform rectangular processing on obstacles and calibration. We rectangular the obstacles and calibration and add black. We can perform grid processing on the blackened map. During the processing, there may be some defects in certain areas, and we can optimize the grid map again. After obtaining a grid map, to facilitate the determination of map location, various regions of the map can be encoded. Each numerical value represents a region.

TABLE 2. Virtual map ant colony algorithm initialization parameter.

Parameter	Parameter value	Significance
K	100	Iterations
M	200	Number of ants
S	62	Starting point
E	3533	Endpoint
Alpha	1.4	Importance of pheromone
Beta	25	Importance of heuristic factors
Rho	0.3	Pheromone evaporation coefficient
Q	1	Pheromone increasing intensity coefficient

Then the relevant parameters are initialized and the path planning of the ant colony algorithm is carried out. After obtaining the planning path and pose parameters, we regress the data to the original non-standard environment map to obtain the planning path and pose of the robot under the non-standard map.

Compared with traditional path planning methods that rely on laser or ultrasonic measurements to obtain grid maps, this improved non-standard map robot path planning method and can achieve robot path planning faster. In addition, it can more intuitively display the planned robot motion path and pose, with more intelligent and humanized characteristics.

B. PRE PROCESSING OF NON-STANDARD MAP

Due to the variability of non-standard environmental conditions, a virtual non-standard map as shown in Figure 3 was designed to better introduce the method. The size and shape of each element in the figure are different. There are a total of 7 elements in the figure, and the circular area in the upper right corner is the calibration object placed for size calibration. The calibration object is very important. Because the size of the map may change during map processing. But because there is a size calibration object, the size of other elements and the size of the entire diagram are all referenced by the calibration object, which ensures the availability of the final obtained data. Here we set the calibration circle part of A actual diameter size of D. If the size of A measured in the picture is d_1 and the size of another object B is d_2, then the actual size of B should be $D \times d_2/d_1$.

The virtual non-standard map in Figure 3 requires a box selection, as shown in Figure 4. Assuming the size range of the box selected is $k \times k$. After the map is box selected, cut it and take out the $k \times k$ part of the map to generate Figure 5. The box selected and cutting process above is also a standardized process for the entire process. For different non-standard maps, we can only grid them into the box to perform non-standard map processing. After cutting, we binarized Figure 5 to obtain Figure 6. The boundary parameters of each obstacle and the set calibration object in Figure 6 were obtained using the regionprops function in Matlab while binarizing the standard map. By using the rectangle function, obstacles and calibration objects are displayed, forming Figure 7.

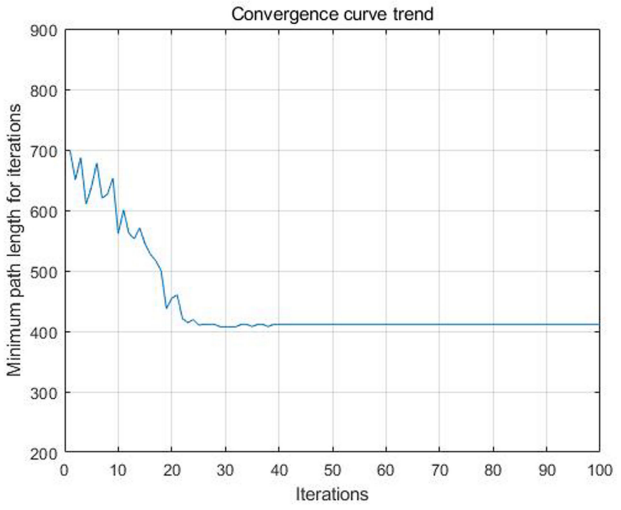

FIGURE 11. Virtual non-standard map safety distance added GM planning path convergence curve.

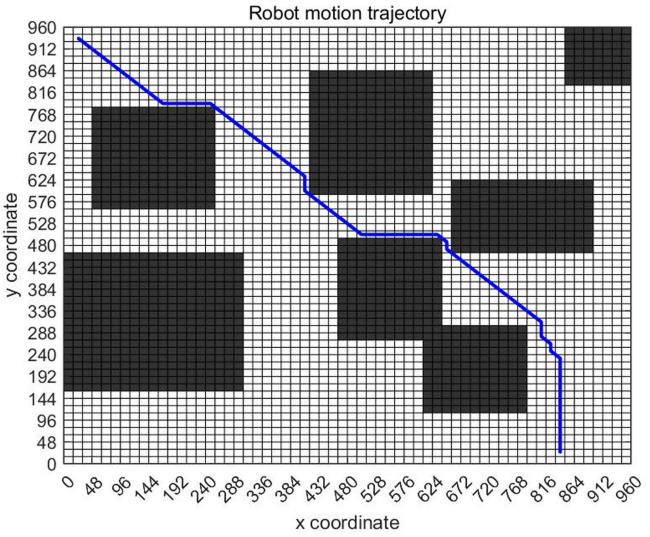

FIGURE 12. Planning path after virtual map improvement.

C. GENERATION OF GRID MAPS

After obtaining Figure 6, a grid map design can be carried out. Separate Figure 6 into $t \times t$ squares. In this way, when the size of the entire map is $b \times b$, the edge length of each grid can be obtained, which is b/t. Then, based on the binarization results, we fill each grid area with a value of 0 in black, and leave the grid area with a value of 1 blank, thus generating the grid map Figure 8. Although we have generated a grid map, we cannot visually view the specific locations of each grid. In this case, we need to encode each grid so that our subsequent path planning will be more convenient.

D. OPTIMIZATION PROCESS

The boundary area of the grid map may become blank due to the influence of dividing the grid strip, as shown in Figure 8. This may lead to collisions between robots and

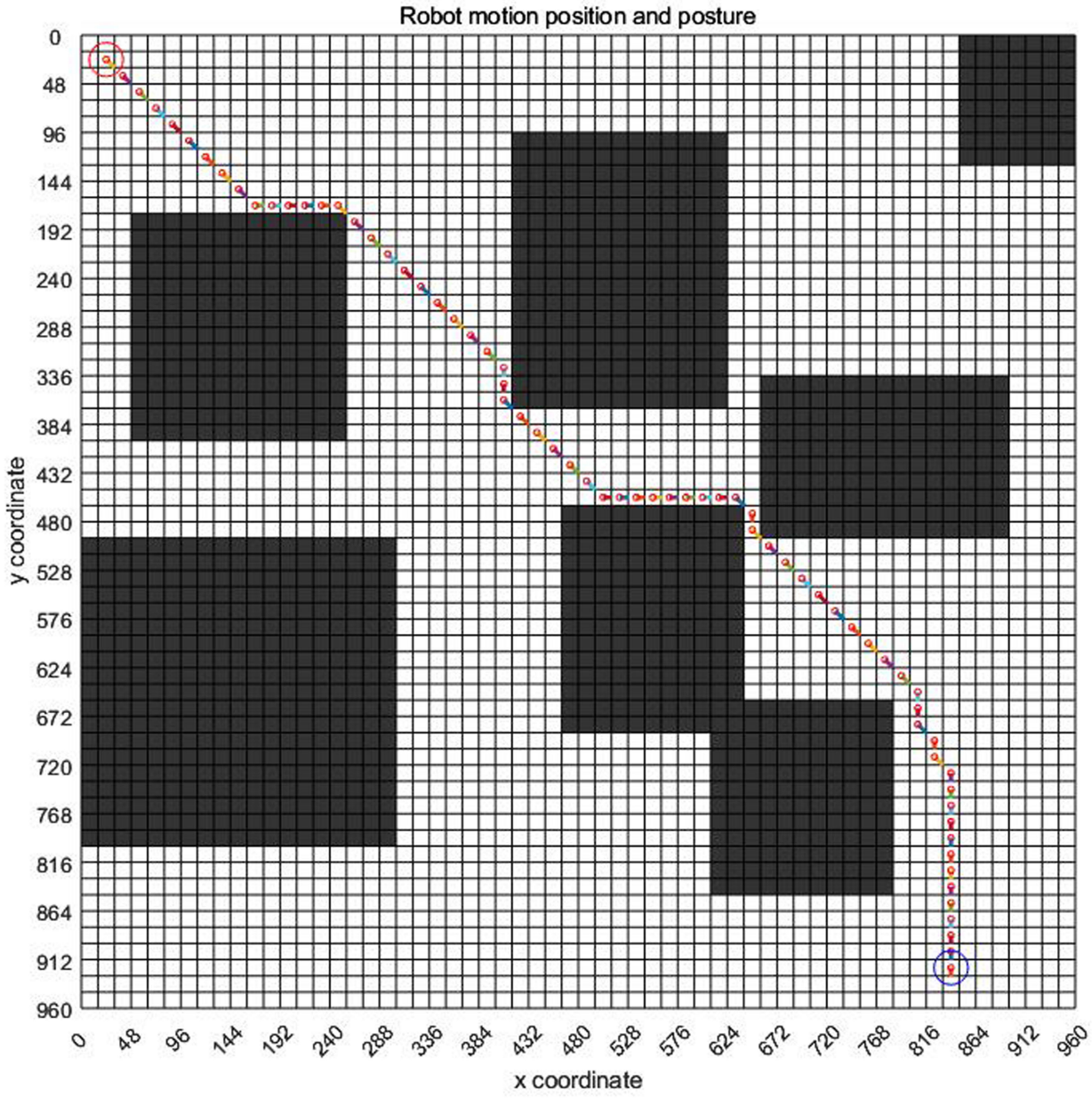

FIGURE 13. Planning pose after virtual map improvement.

obstacles during subsequent path planning. To avoid contact between robots and obstacles, we need to optimize the map. We can expand the black grid area to ensure the safety of the robot. we have generated black rectangular blocks of obstacles through the bounding boxes selected in Figure 7. These rectangular blocks can be set as external to or larger than the obstacle in the original image, and can fully cover the obstacle. Here we can add a safety distance P, and then reconstruct the map, as shown in Figure 9(c). This distance P can be set according to the structure of the robot itself or according to the safety needs. In this way, we once again ensure the safety of the robot's moving path in the real environment.

In the following, we take Figure 9 (c) as an example for path planning. Figure 9 (c) is more standardized than Figure 9 (a). Again, binarize Figure 9 (c) and perform grid partitioning to obtain Figure 10 (a). The arrows in Figure 10 (a) indicate that some areas have not been blackened out due to the size issue of the grid division area. We need to continue processing the grid and reset the value to 0 at these points, thus forming an optimized map as shown in Figure 10 (b).

In this way, we optimized the map through non-standard map processing. The optimized grid map 10 (b) is more standard and more suitable for path planning with the ant colony algorithm.

TABLE 3. Real environment map ant colony algorithm initialization parameter.

Parameter	K	M	*Alpha*	*Beta*	*Rho*	Q	S	E
Value	100	200	1.4	20	0.3	1	62	3533

E. ANT COLONY ALGORITHM IMPLEMENTATION

Ant colony algorithm is an intelligent path-planning method. When an ant goes to find food, a place as the starting point, and then goes to all other places one by one. The ant can volatilize pheromone in the process of looking for food and finally return to the starting point [43], [44]. Assuming there are N locations and their directed graph is $G(N, A)$, and

$$N = \{1, 2, 3, 4 \ldots, n-1, n\},$$
$$A = \{(i, j)|i, j \in N\},$$

Let the distance between two points be $(l_{ij})_{n\times n}$. The length of the ant's path is:

$$f(w) = \sum_{l=1}^{n} l_{i_{l-1}} l_{i_l} \tag{1}$$

in which

$$w = (i_1, i_2, i_3, i_4 \cdots i_{n-1}, i_n),$$

In the algorithm, the ant needs to go from one point to another based on the probability of reaching the next point. The probability is:

$$P_{ij}^{k}(t) = \frac{\left[\tau_{ij}(t)\right]^{\alpha} \times \left[\eta_{ij}(t)\right]^{\beta}}{\sum_{k \in allowd_k} \left[\tau_{ij}(t)\right]^{\alpha} \times \left[\eta_{ij}(t)\right]^{\beta}} \tag{2}$$

i, j is the starting point and target point of ants,

$$\eta_{ij} = 1/l_{ij} \tag{3}$$

η_{ij} is visibility, which is the reciprocal of the distance between i and j, $\tau_{ij}(t)$ refers to the pheromone from i to j at time t, $allowed_k$ is a collection of locations that ants have never visited, a, β is the weighted value of pheromone and visibility.

The pheromone is constantly updated and can be expressed as follows:

$$\tau_{ij}(t) = (1-\rho)\tau_{ij}(t) + \sum_{k=1}^{m} \tau_{ij}^{k} \tag{4}$$

m is the number of ants.

$\Delta\tau_{ij}^{k}$ is the pheromone left by the k-th ant when it moves from i to j,

$$\Delta\tau_{ij}^{k} = 1/C_k \tag{5}$$

Among them, i, j is the point passing by the ant, C_k is the total length of the path obtained by the k-th ant walking the entire path.

Through the above process, ants walk through the path. We perform iterative operations continuously based on the settings.

The main parameters of the ant colony algorithm are the number of iterations, the number of ants, the starting point, the endpoint, the pheromone importance coefficient, the heuristic factor importance coefficient, the pheromone evaporation coefficient, etc. Since the ant colony algorithm plans the path through a grid to grid motion planning, a grid map is very suitable for the operation of ant colony algorithm.

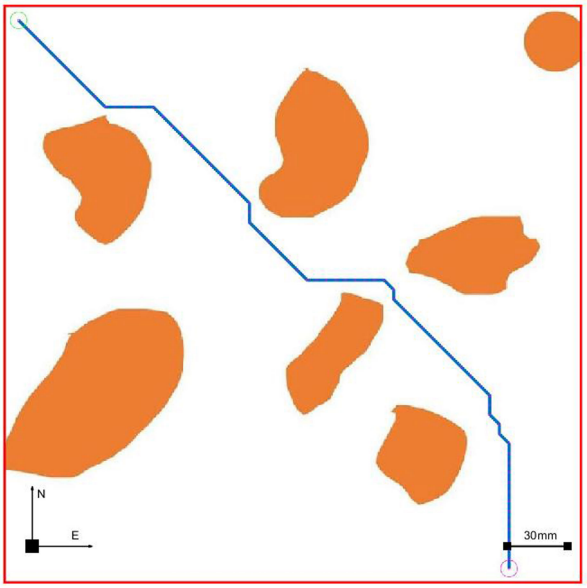

FIGURE 14. Virtual non-standard map planning path.

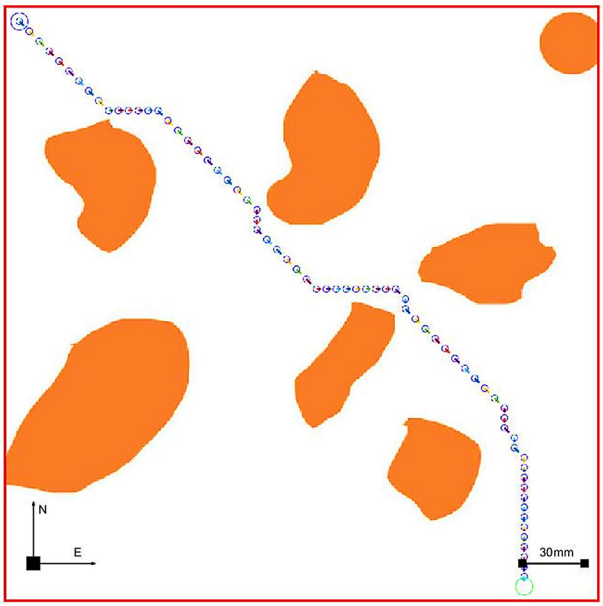

FIGURE 15. Virtual non-standard map planning pose.

FIGURE 16. Non-standard real environment map.

FIGURE 17. Non-standard map box selected.

FIGURE 18. Non-standard map cropping.

FIGURE 19. Calibration object.

F. ROBOT MOTION TRAJECTORY SIMULATION

After getting a grid map, we can plan the path through the ant colony algorithm. According to the encoding in Figure 10 (c), we can set the initial position and end point of the virtual map. The ant colony algorithm path planning parameters are as Table 2.

The convergence curves after optimization in Figure 11 prove that the proposed method is theoretically feasible and can achieve path planning for mobile robots in non-standard maps.

Figure 12 is the path obtained by the ant colony algorithm. After 100 iterations, the blue route on the map is the planning path. Through 71 points, the ants passed 62-123-184—3413-3473-3533, and eventually bypassed obstacles smoothly to reach the target location.

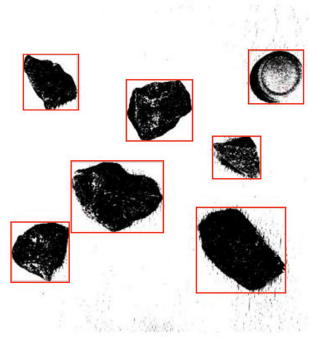

FIGURE 20. Non-standard map obstacle box selected.

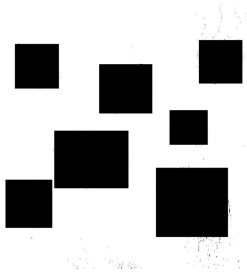

FIGURE 21. Non-standard map obstacle rectangle without safety distance box selected.

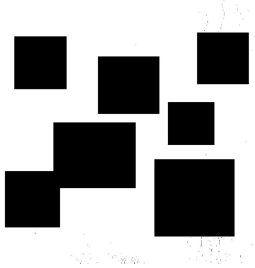

FIGURE 22. Non-standard map obstacle rectangle after box selected and safety distance added.

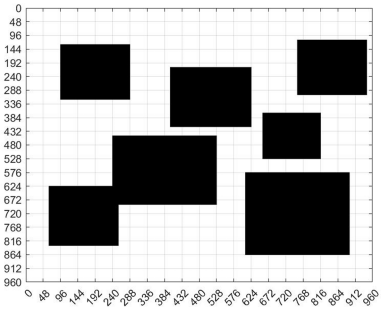

FIGURE 23. Grid map after improvement of non-standard map.

If the planning path is R, $R = \{R_1, R_2, \ldots, R_i, \ldots, R_n\}$, $i \in [1, n]$, where R_1 is the initial point and R_n is the target point. The coordinates of each point R_i is (x_i, y_i), then the planning path point group coordinate formula C is

$$C = \{(x_1, y_1), (x_2, y_2) \ldots, (x_i, y_i), \ldots, (x_n, y_n)\},$$

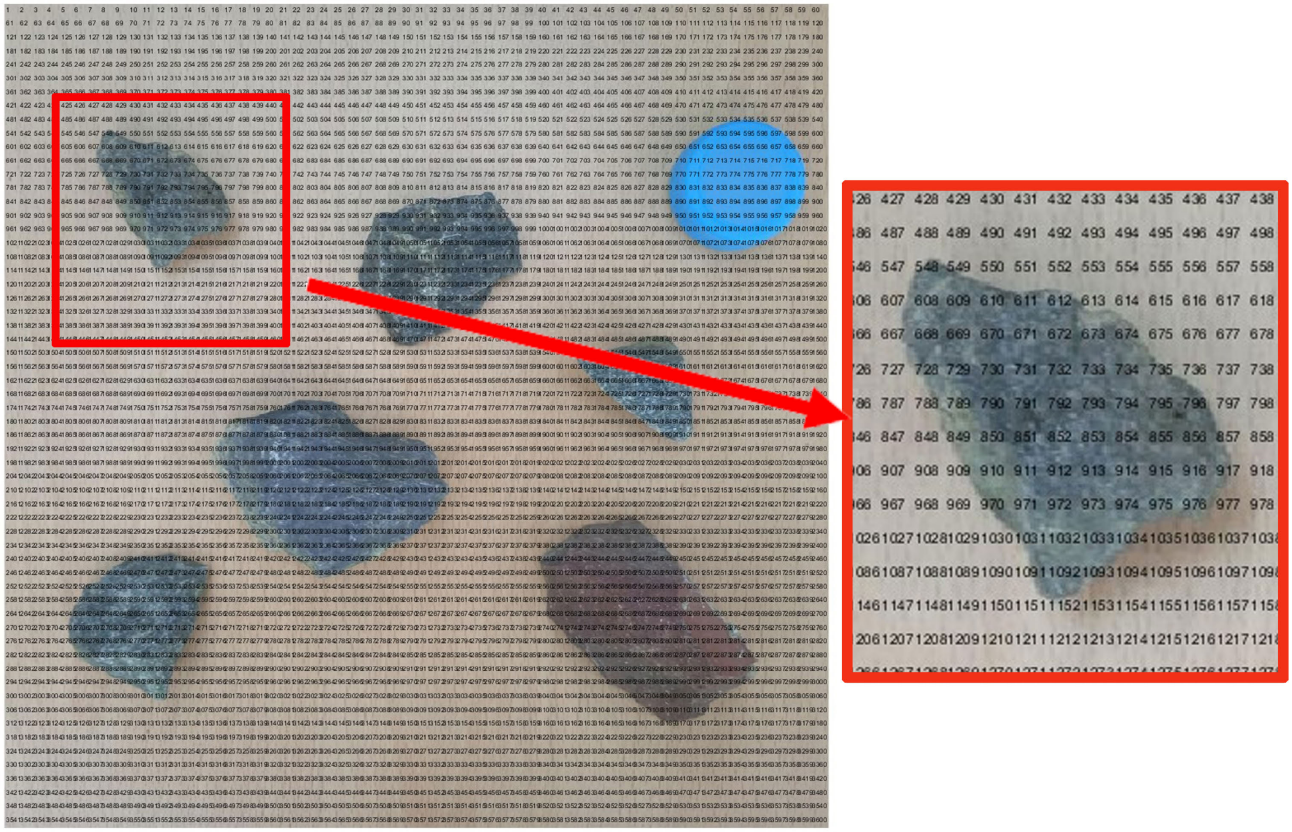

FIGURE 24. Non-standard map Encoding.

The distance of each part is $L_{Ri,Ri+1}$,

$$L_{R_i,R_{i+1}} = \sqrt{(x_{i+1} - x_i)^2 + (y_{i+1} - y_i)^2},\ i \in [1, n-1] \tag{6}$$

The total path length is L,

$$L = \sum_1^{n-1} L_{R_i,R_{i+1}} = L_{R_1,R_2} + L_{R_2,R_3} + L_{R_3,R_4} + \ldots + L_{R_{n-1},R_n} \tag{7}$$

And each point pose is $\beta_{Ri,Ri+1}$,

$$\beta_{R_i,R_{i+1}} = \frac{y_{i+1} - y_i}{x_{i+1} - x_i}, \quad i \in [1, n-1] \tag{8}$$

According to the planning path parameters, the planning pose as Figure 13 can be obtained. The small circle in the figure represents the position of the ant, and the straight line in the circle represents the ant's pose when preparing to move toward the next point at its current position.

After obtaining the planning path parameters of the mobile robot, the planning path parameters need to be returned to the original non-standard maps, as shown in Figure14. Due to the existence of the size calibration in the figure, we can get the real location of the ants in the virtual map with a scale. We can also add coordinates in the vertical and horizontal axis of the figure so that the positions of each point can be better displayed.

Based on the planning path and pose data in Figures 12-13, we regress these data to the non-standard map, as shown in Figures 14 and 15. In Figure 14-15, the ant's movement path, pose and environment are clear at a glance, which has significant advantages compared to the traditional grid map representations in Figure 12.

VI. EXPERIMENTAL VERIFICATION

In this chapter, we will introduce the application of the proposed method on a non-standard real environment map. We describe the problems encountered in the standardization design of non-standard real environment maps. We optimized the grid map and planned the path of the non-standard map in the real environment through the ant colony algorithm.

A. NON-STANDARD MAP

As shown in Figure 16, there are 6 obstacles and a calibration object. The color of the calibration object is lighter. It is light blue. Put it in the upper right corner of the map. This map is shown in Matlab as 3120 × 4160 pixels. The actual diameter of the calibration is 30 mm (Figure 19). Figure 17 shows the box selected of non-standard maps. Select the size of the box 960 × 960. After the box is selected, the image is cut into Figure 18.

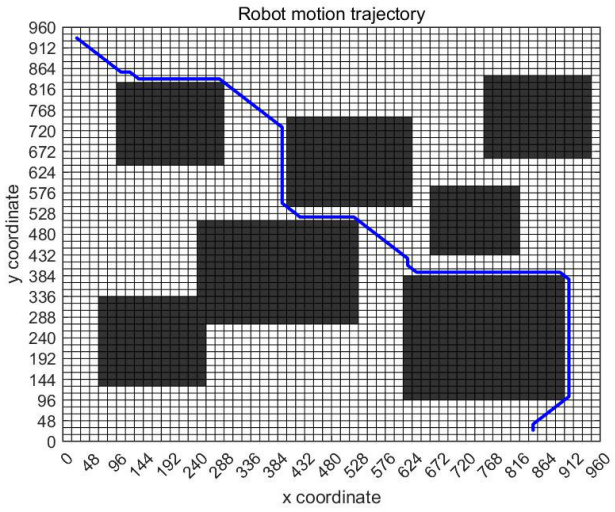

FIGURE 25. The planning path after the improvement of the non-standard map.

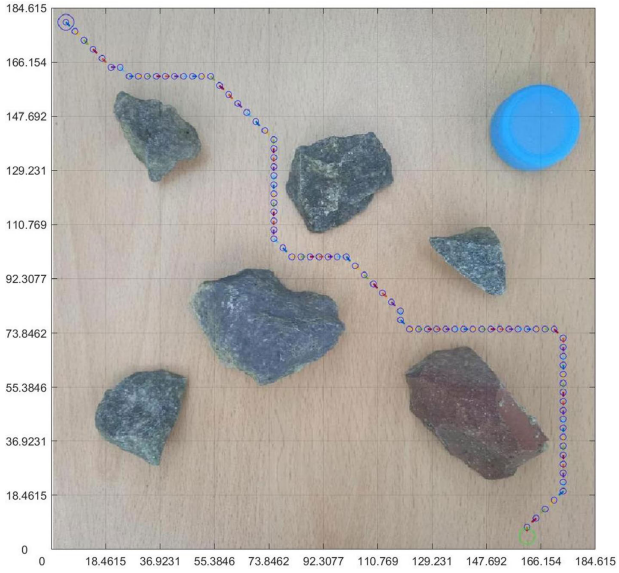

FIGURE 26. The planning pose after the improvement of the non-standard map.

B. STANDARDIZED DESIGN

Figure 20 shows the binarization and box selected result of Figure 18. According to the method proposed in the previous text, we box-selected obstacles in non-standard maps to obtain the size parameters of the non-standard map. After querying the parameters, the diameter of the calibration in the system is 157, so the scale is $Z = 157 / 30 = 5.2333$.

Figure 21 shows obstacle rectangle without safety distance after the box selected. It can be seen from the figure that all obstacles have been covered, but the box selected is a rectangle formed according to the maximum size of the obstacle itself. To ensure the absolute safety of the robot's planning path, we can add a safety distance. Here, we set the safety size P as 3mm, and then the corresponding size inside the system is $3 \times Z = 3 \times 5.2333 = 15.6999$. Then, we cover the obstacles again in a rectangular way, and Figure 22 is generated

C. ANT COLONY IMPLEMENTATION

According to the non-standard map coding in Figure 24, we can accurately obtain the corresponding codes for each position on the map. By inputting the initial and endpoint positions, we can easily obtain the robot planning route and pose according to the method proposed in this article. we set the starting position of the ants as point 62 and the final target position as point 3533. The number of iterations is 100, and the number of ants is 200. The parameter settings for this non-standard map of the actual environment are shown in Table 3.

D. EXPERIMENTAL RESULTS ANALYSIS COMPARISON

Figure 25 shows the planning path generated in the grid map Figure 23. It is the planning path obtained through 100 iterations of ant colony algorithms according to the initialization parameters. In the picture, the ants successfully arrived at

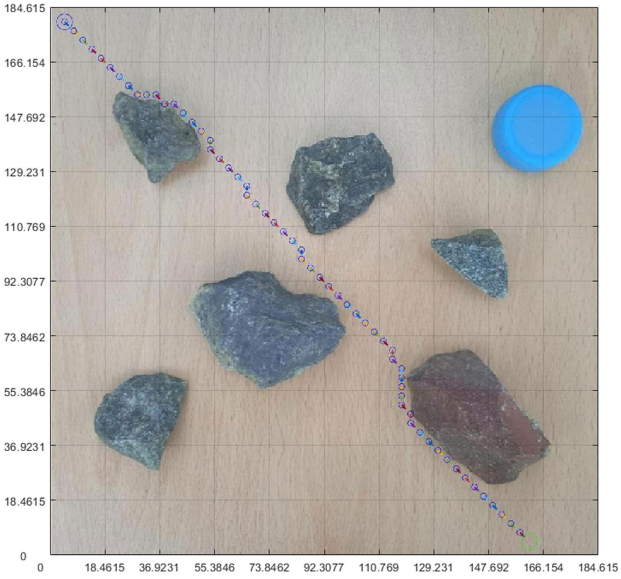

FIGURE 27. The planning pose of the original non-standard map.

the target point from the initial point after passing through each node in the route. The picture again confirmed that the method proposed in this paper is feasible and can achieve path planning after standardizing the non-standard map. Since the obstacles in Figure 25 are processed by adding the safety distance, it can be seen from the figure that the distance from the route to the obstacles becomes a little farther. This avoids the possibility of robots colliding with obstacles in some areas due to the grid process during the map standardization, thus, the safety of the planning path is guaranteed.

We returned the planning path data in Figure 25 to the real environment non-standard map, carried out pose planning and design, and obtained Figure 26. Figure 26 shows the various

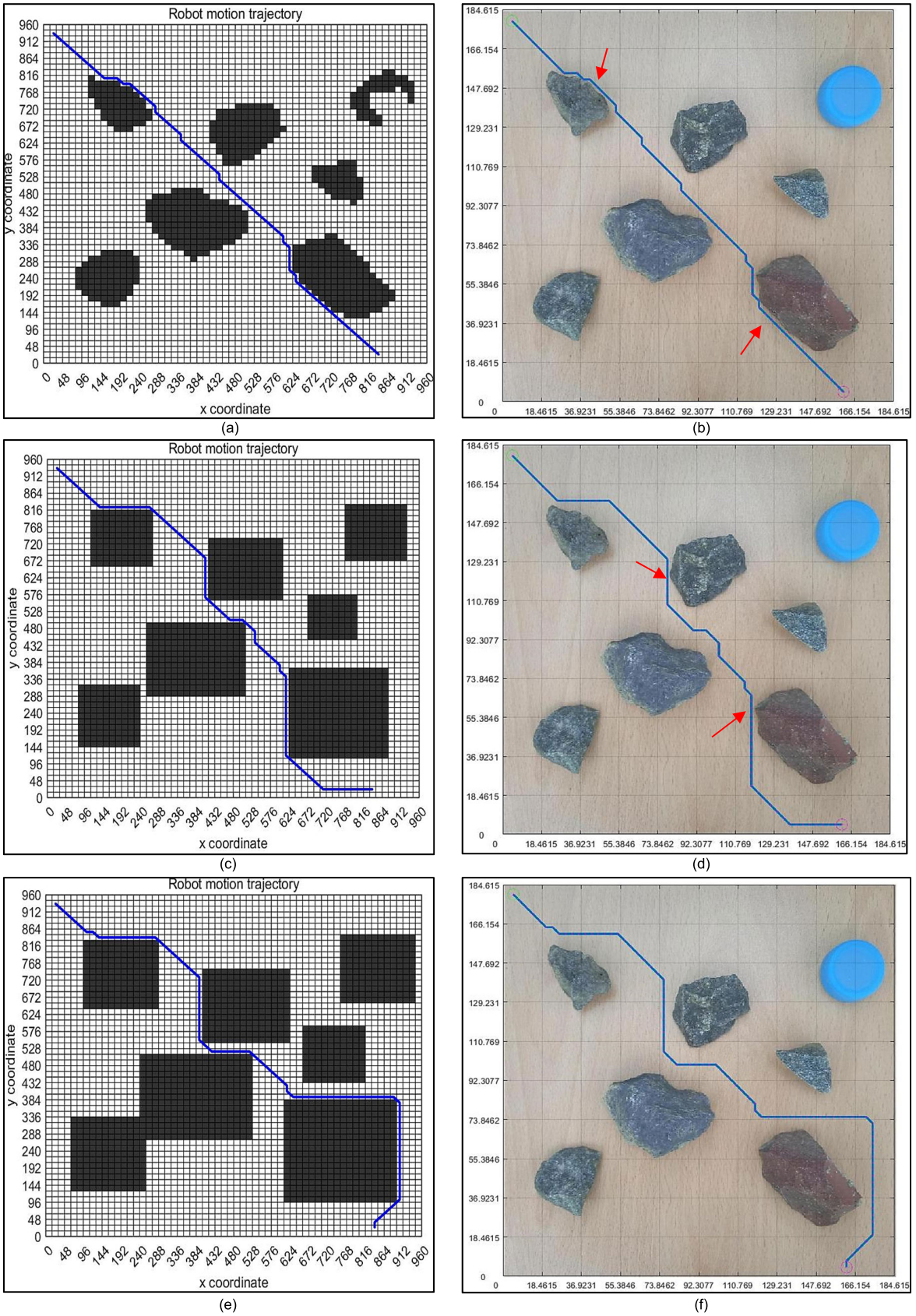

FIGURE 28. Comparison of planning paths. (a) Original unoptimized GM planning path. (b) Original unoptimized real environment map planning path. (c) No safety distance added obstacle box selected GM planning path. (d) No safety distance added obstacle box selected real environment planning path. (e) Safety distance added obstacle box selected GM planning path. (f) Safety distance added obstacle box selected real environment planning path.

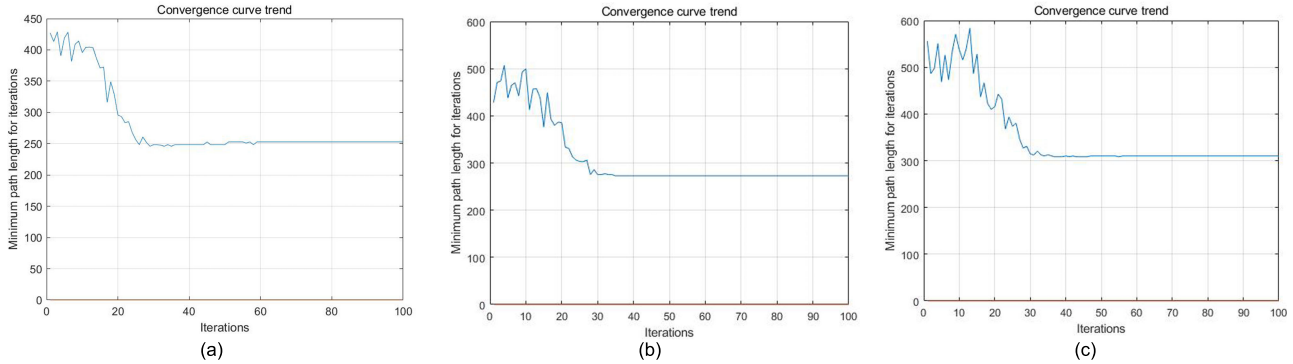

FIGURE 29. Comparison of convergence curves. (a) Original unoptimized GM planning path convergence curve. (b) No safety distance added obstacle box selected GM planning path convergence curve. (c) Safety distance added obstacle box selected GM planning path convergence curve.

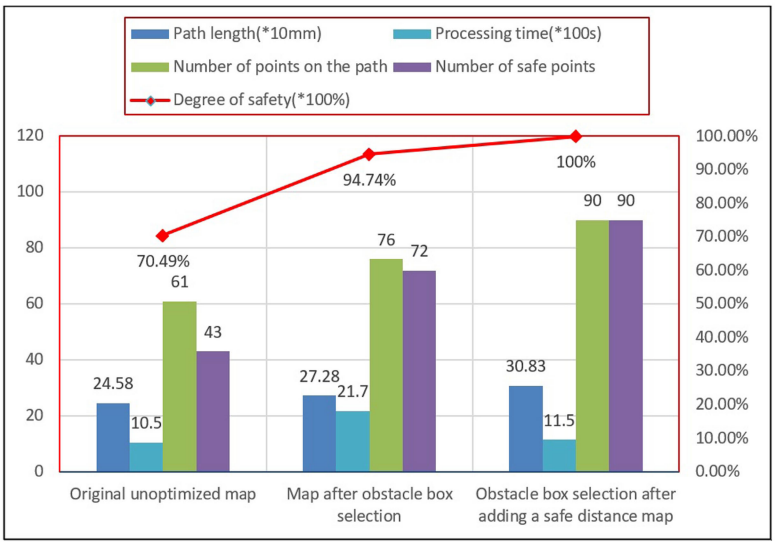

FIGURE 30. Comparison of path planning results of ant colony algorithm in real environment.

positions and poses of the robot movement. The positions and poses in the figure are visible, intuitive, easy to understand, and well reflect the ant's walking state. The small circles in the figure represent the positions that the robot needs to walk through, and the straight lines in the circles point to the posture that the robot needs to reach. Figure 27 is the planning pose of the original non-standard map, it can be seen from the figure that there are many points in the planning path that are very close to the obstacles, which may lead to the robot and the obstacle touching, which is dangerous for the robot. Compared with Figure 27, it can be seen that the distance between the planning path and the obstacles in Figure 26 is very appropriate. This ensures the good operation of the robot. In the figures, the relationship between the robot's motion planning path and obstacles is very clear. Relative to traditional grid map robot planning paths like Figure 25, the method described in this article can better reflect the real motion control scheme of the robot and has a wider application prospect.

E. ANALYSIS AND COMPARISON OF THE THREE METHOD RESULTS

In this section, to further prove the superior performance of the ant colony algorithm planning path in the real environment proposed in this paper, the original unoptimized GM planning path, no safety distance added obstacle box selected planning path, and safety distance added obstacle box selected planning path are given.

As shown in Figure 28(a)~(f), it can be seen from the six figures that the ant colony algorithm can be used to realize the path planning in the real environment under the existing parameters. However, it can be seen from the original unoptimized GM planning path in Figure 28(b) and the no safety distance added obstacle box selected planning path in Figure 28(d) that some paths are dangerous areas because they are very close to the obstacles. In the no safety distance added obstacle box selected planning path in Figure 28(f), it is obvious that the whole path is safe.

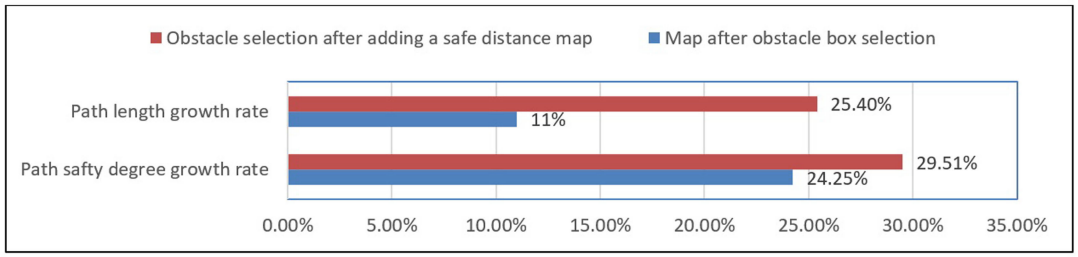

FIGURE 31. Comparison of path planning results of ant colony algorithm in real environment.

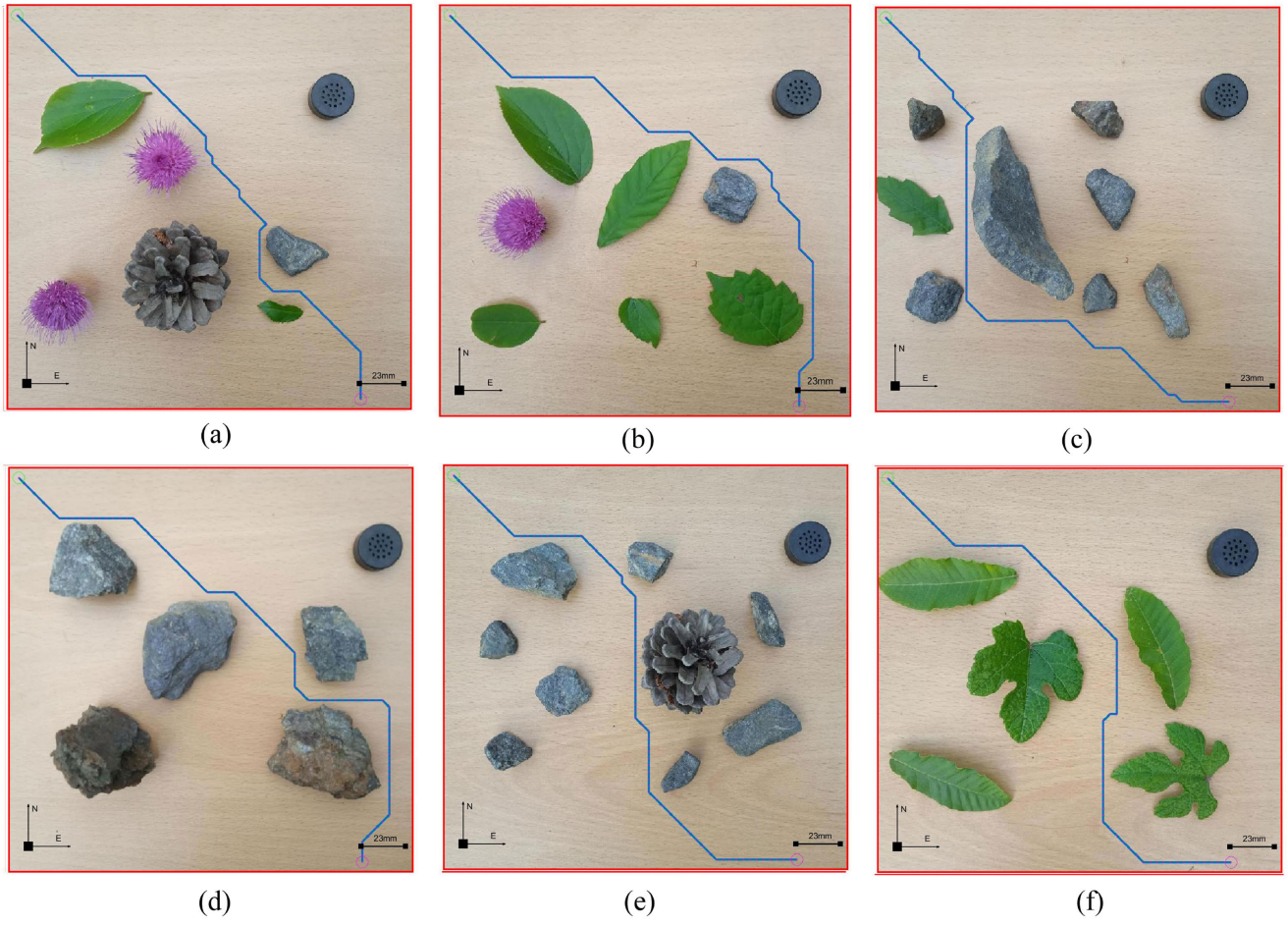

FIGURE 32. Different environmental path planning. (a) Environment 1. (b) Environment 2. (c) Environment 3. (d) Environment 4. (e) Environment 5. (f) Environment 6.

Figure 29 shows the original unoptimized, no safety distance added obstacle box selected and safety distance added obstacle box selected GM planning path convergence curves. We can get the relevant parameters of the ant colony algorithm operation in three cases through the three curves. According to the relevant parameters, combined with Figure 28, We obtained the relevant data and compared the path planning of the three methods with the relevant data.

It can be seen from Figure 30 that the path and processing time planned by the original grid map are the shortest, which are 245.8mm and 1050s respectively. The planning path length and processing time of no safety distance added obstacle box selected GM and safety distance added obstacle box selected GM have been increased. As can be seen from Figure 31, in the three groups of experiments, the path length planned by the ant colony algorithm increased by 11% after no safety distance added obstacle box selected, and the path length increased by 25.4% after safety distance added obstacle box selected to plan the path. However, the number of safety points on the whole path of the two methods increased

by 24.25% and 29.51% respectively, especially after adding a safety distance, the number of safety points on the whole path reached 100%, which is completely safe. This safety distance added obstacle box selected GM path planning ensures the safety degree of the planning path of the ant colony algorithm under the real environment map.

F. REPEATED IMPLEMENTATION

Then we used the method described in this paper to carry out path planning for multiple non-standard real environment maps, as shown in Figure 32 (a)∼(f), which achieved the purpose of ant colony algorithms after the standardized design of improved non-standard environment maps. From several figures, it can be seen that this method can not only obtain specific parameters for robot path planning but also visually display the robot's motion path and status. The expression effect is very well.

VII. CONCLUSION

Aiming at the problems in the path planning algorithm of robot ant colony algorithm, such as difficult map making, weak intuitiveness, and weak reflection to the real environment in robot path planning, a method is proposed to process non-standard real environment maps, obtain grid standard maps, and modify the grid maps to achieve and optimize real environment path planning. The main contributions of this method are as follows:

1) The standardized design of a non-standard real environment map is proposed to form a grid map, which can be applied to ant colony algorithm for path planning and pose planning.
2) Add a calibration object in the real environment to facilitate changes in size during map processing, ensuring that the final displayed size can reflect the true size.
3) The processing of the non-standard map is optimized by adding safety distance to the obstacle box selected, and the safety degree of the generated planning path is increased by 29.51% compared with the path generated under the original non-standard map, which ensures the safety of the planning path.
4) The planning path and pose are finally restored to the original non-standard map, intuitively displaying the motion path and pose in the real environment, for the convenience of robot motion path planning in different environments.

We have repeatedly verified the effectiveness of this method through multiple experiments. The method proposed in this paper can solve the path planning problem of mobile robots in real environment maps, and greatly improve the intelligent level of robot motion control.

DECLARATION OF COMPETING INTEREST

The authors declare that they have no known competing financial interests or personal relationships that could have appeared to influence the work reported in this paper.

REFERENCES

[1] W. Hou, Z. Xiong, C. Wang, and H. Chen, "Enhanced ant colony algorithm with communication mechanism for mobile robot path planning," *Robot. Auto. Syst.*, vol. 148, Feb. 2022, Art. no. 103949, doi: 10.1016/j.robot.2021.103949.

[2] M. Zhao, H. Lu, S. Yang, and F. Guo, "The experience-memory Q-learning algorithm for robot path planning in unknown environment," *IEEE Access*, vol. 8, pp. 47824–47844, 2020, doi: 10.1109/ACCESS.2020.2978077.

[3] J. Zhao, S. Liu, and J. Li, "Research and implementation of autonomous navigation for mobile robots based on SLAM algorithm under ROS," *Sensors*, vol. 22, no. 11, p. 4172, May 2022, doi: 10.3390/s22114172.

[4] L. Liu, B. Wang, and H. Xu, "Research on path-planning algorithm integrating optimization A-star algorithm and artificial potential field method," *Electronics*, vol. 11, no. 22, p. 3660, Nov. 2022, doi: 10.3390/electronics11223660.

[5] S. Wang, Z. Ren, and M. Wu, "Non-uniform input-based adaptive growing neural gas for unstructured environment map construction," *Appl. Sci.*, vol. 12, no. 12, p. 6110, Jun. 2022, doi: 10.3390/app12126110.

[6] J. Guo, X. Jin, S. Guo, and Q. Fu, "A vascular interventional surgical robotic system based on force-visual feedback," *IEEE Sensors J.*, vol. 19, no. 23, pp. 11081–11089, Dec. 2019, doi: 10.1109/JSEN.2019.2935002.

[7] T. Linner, W. Pan, R. Hu, C. Zhao, K. Iturralde, M. Taghavi, J. Trummer, M. Schlandt, and T. Bock, "A technology management system for the development of single-task construction robots," *Construct. Innov.*, vol. 20, no. 1, pp. 96–111, Jan. 2020, doi: 10.1108/CI-06-2019-0053.

[8] A. Dhiman, N. Shah, P. Adhikari, S. Kumbhar, I. S. Dhanjal, and N. Mehendale, "Firefighting robot with deep learning and machine vision," *Neural Comput. Appl.*, vol. 34, no. 4, pp. 2831–2839, Feb. 2022, doi: 10.1007/s00521-021-06537-y.

[9] Z. Huang, L. He, Z. Gao, Y. Jia, Y. Kang, D. Xie, and C. Fu, "Research on spatial positioning of online inspection robots for vertical storage tanks," *Ind. Robot: Int. J. Robot. Res. Appl.*, vol. 47, no. 2, pp. 187–195, Dec. 2019, doi: 10.1108/IR-08-2019-0168.

[10] Y. Ou, P. Yin, and L. Mo, "An improved grey wolf optimizer and its application in robot path planning," *Biomimetics*, vol. 8, no. 1, p. 84, Feb. 2023, doi: 10.3390/biomimetics8010084.

[11] Y. Mu, B. Li, D. An, and Y. Wei, "Three-dimensional route planning based on the beetle swarm optimization algorithm," *IEEE Access*, vol. 7, pp. 117804–117813, 2019, doi: 10.1109/ACCESS.2019.2935835.

[12] L. Yang, Q. He, L. Yang, and S. Luo, "A fusion multi-strategy marine predator algorithm for mobile robot path planning," *Appl. Sci.*, vol. 12, no. 18, p. 9170, Sep. 2022, doi: 10.3390/app12189170.

[13] Y. Zhang, G. Guan, and X. Pu, "The robot path planning based on improved artificial fish swarm algorithm," *Math. Problems Eng.*, vol. 2016, pp. 1–11, Aug. 2016, doi: 10.1155/2016/3297585.

[14] L. Cao, K. Ben, H. Peng, and X. Zhang, "Enhancing firefly algorithm with adaptive multi-group mechanism," *Int. J. Speech Technol.*, vol. 52, no. 9, pp. 9795–9815, Jul. 2022, doi: 10.1007/s10489-021-02766-9.

[15] Y. Chen, B. Tan, and L. Zeng, "Inspection path planning of free-form surfaces based on improved cuckoo search algorithm," *Meas. Control*, vol. 56, nos. 7–8, pp. 1321–1332, Sep. 2023, doi: 10.1177/00202940231157422.

[16] K. Konolige, "Improved occupancy grids for map building," *Auto. Robots*, vol. 4, no. 4, pp. 351–367, 1997, doi: 10.1023/A:1008806422571.

[17] M.-S. Yuan, T.-L. Zhou, and M. Chen, "Improved lazy theta* algorithm based on octree map for path planning of UAV," *Defence Technol.*, vol. 23, pp. 8–18, May 2023, doi: 10.1016/j.dt.2022.01.006.

[18] C. Choe, S. Ahn, N. Doh, and C. Nam, "Reduction of LiDAR point cloud maps for localization of resource-constrained robotic systems," *IEEE Syst. J.*, vol. 17, no. 1, pp. 916–927, Mar. 2023, doi: 10.1109/JSYST.2022.3162926.

[19] D. Zhang, Y.-B. Yin, R. Luo, and S.-L. Zou, "Hybrid IACO–A*-PSO optimization algorithm for solving multiobjective path planning problem of mobile robot in radioactive environment," *Prog. Nucl. Energy*, vol. 159, May 2023, Art. no. 104651, doi: 10.1016/j.pnucene.2023.104651.

[20] Y. Chen, J. Wu, C. He, and S. Zhang, "Intelligent warehouse robot path planning based on improved ant colony algorithm," *IEEE Access*, vol. 11, pp. 12360–12367, 2023, doi: 10.1109/ACCESS.2023.3241960.

[21] C. Gong, Y. Yang, L. Yuan, and J. Wang, "An improved ant colony algorithm for integrating global path planning and local obstacle avoidance for mobile robot in dynamic environment," *Math. Biosci. Eng.*, vol. 19, no. 12, pp. 12405–12426, 2022, doi: 10.3934/mbe.2022579.

[22] C. Huang, Z. Gao, J. Chen, L. Zhou, Z. Lu, and Q. Qu, "Guide circle-based improved ant colony algorithm," *J. Phys., Conf. Ser.*, vol. 1634, no. 1, Sep. 2020, Art. no. 012057, doi: 10.1088/1742-6596/1634/1/012057.

[23] C. V. Dang, H. Ahn, D. S. Lee, and S. C. Lee, "Improved analytic expansions in hybrid A-star path planning for non-holonomic robots," *Appl. Sci.*, vol. 12, no. 12, p. 5999, Jun. 2022, doi: 10.3390/app12125999.

[24] X. Wang, X. Ma, and Z. Li, "Research on SLAM and path planning method of inspection robot in complex scenarios," *Electronics*, vol. 12, no. 10, p. 2178, May 2023, doi: 10.3390/electronics12102178.

[25] Y. Ou, Y. Fan, X. Zhang, Y. Lin, and W. Yang, "Improved A* path planning method based on the grid map," *Sensors*, vol. 22, no. 16, p. 6198, Aug. 2022, doi: 10.3390/s22166198.

[26] A. Choudhary, "Sampling-based path planning algorithms: A survey," 2023, *arXiv:2304.14839*.

[27] S. Kumar and A. Sikander, "A novel hybrid framework for single and multi-robot path planning in a complex industrial environment," *J. Intell. Manuf.*, Dec. 2022, doi: 10.1007/s10845-022-02056-2.

[28] L. Qiao, X. Luo, and Q. Luo, "An optimized probabilistic roadmap algorithm for path planning of mobile robots in complex environments with narrow channels," *Sensors*, vol. 22, no. 22, p. 8983, Nov. 2022, doi: 10.3390/s22228983.

[29] X. Xia, T. Li, S. Sang, Y. Cheng, H. Ma, Q. Zhang, and K. Yang, "Path planning for obstacle avoidance of robot arm based on improved potential field method," *Sensors*, vol. 23, no. 7, p. 3754, Apr. 2023, doi: 10.3390/s23073754.

[30] S. Chehelgami, E. Ashtari, M. A. Basiri, M. T. Masouleh, and A. Kalhor, "Safe deep learning-based global path planning using a fast collision-free path generator," *Robot. Auto. Syst.*, vol. 163, May 2023, Art. no. 104384, doi: 10.1016/j.robot.2023.104384.

[31] A. Özdemir and S. O. Bogosyan, "Gap based elastic trees as a novel approach for fast and reliable obstacle avoidance for UGVs," *J. Intell. Robotic Syst.*, vol. 107, no. 1, p. 9, Jan. 2023, doi: 10.1007/s10846-022-01792-0.

[32] K. S. Suresh, K. S. Ravichandran, and S. Venugopal, "Multi-objective genetic algorithm for mobile robot path planning in industrial automation," *J. Intell. Fuzzy Syst.*, vol. 44, no. 4, pp. 6829–6842, Apr. 2023, doi: 10.3233/JIFS-220886.

[33] K. S. Suresh, R. Venkatesan, and S. Venugopal, "Mobile robot path planning using multi-objective genetic algorithm in industrial automation," *Soft Comput.*, vol. 26, no. 15, pp. 7387–7400, Aug. 2022, doi: 10.1007/s00500-022-07300-8.

[34] Z. Yu, L. Zhang, and J. Kim, "The performance analysis of PSO-ResNet for the fault diagnosis of vibration signals based on the pipeline robot," *Sensors*, vol. 23, no. 9, p. 4289, Apr. 2023, doi: 10.3390/s23094289.

[35] S. Dian, J. Zhong, B. Guo, J. Liu, and R. Guo, "A smooth path planning method for mobile robot using a BES-incorporated modified QPSO algorithm," *Expert Syst. Appl.*, vol. 208, Dec. 2022, Art. no. 118256, doi: 10.1016/j.eswa.2022.118256.

[36] F. Gul, I. Mir, D. Alarabiat, H. M. Alabool, L. Abualigah, and S. Mir, "Implementation of bio-inspired hybrid algorithm with mutation operator for robotic path planning," *J. Parallel Distrib. Comput.*, vol. 169, pp. 171–184, Nov. 2022, doi: 10.1016/j.jpdc.2022.06.014.

[37] X. Hu, Y. Shi, G. Bai, and Y. Chen, "Collaborative search and target capture of AUV formations in obstacle environments," *Appl. Sci.*, vol. 13, no. 15, p. 9016, Aug. 2023, doi: 10.3390/app13159016.

[38] M. Natarajan et al., "Human-robot teaming: Grand challenges," *Current Robot. Rep.*, Aug. 2023, doi: 10.1007/s43154-023-00103-1.

[39] L. Liu, X. Wang, X. Yang, H. Liu, J. Li, and P. Wang, "Path planning techniques for mobile robots: Review and prospect," *Expert Syst. Appl.*, vol. 227, Oct. 2023, Art. no. 120254, doi: 10.1016/j.eswa.2023.120254.

[40] Y. Sun, C. Zhang, and C. Liu, "Collision-free and dynamically feasible trajectory planning for omnidirectional mobile robots using a novel B-spline based rapidly exploring random tree," *Int. J. Adv. Robotic Syst.*, vol. 18, no. 3, May 2021, Art. no. 172988142110166, doi: 10.1177/17298814211016609.

[41] H. Tang, A. Lin, W. Sun, and S. Shi, "An improved SOM-based method for multi-robot task assignment and cooperative search in unknown dynamic environments," *Energies*, vol. 13, no. 12, p. 3296, Jun. 2020, doi: 10.3390/en13123296.

[42] Y. Liu, M. J. Er, and C. Guo, "Online time-optimal path and trajectory planning for robotic multipoint assembly," *Assem. Autom.*, vol. 41, no. 5, pp. 601–611, Sep. 2021, doi: 10.1108/AA-03-2021-0029.

[43] R. Fardel, M. Nagel, F. Nüesch, T. Lippert, and A. Wokaun, "Fabrication of organic light-emitting diode pixels by laser-assisted forward transfer," *Appl. Phys. Lett.*, vol. 91, no. 6, Aug. 2007, Art. no. 061103, doi: 10.1063/1.2759475.

[44] J. Zhang and N. Tansu, "Optical gain and laser characteristics of InGaN quantum wells on ternary InGaN substrates," *IEEE Photon. J.*, vol. 5, no. 2, Apr. 2013, Art. no. 2600111, doi: 10.1109/JPHOT.2013.2247587.

FENG LI received the B.Eng. and M.Eng. degrees in mechanical engineering from the Zhongyuan University of Technology, China, in 2007 and 2010, respectively. He is currently pursuing the Ph.D. degree with Kunsan National University, South Korea. He is also an associate professor. His research interests include robot motion control and artificial intelligence.

YOUNG-CHUL KIM received the B.Eng. and M.Eng. degrees in electrical engineering from Chonbuk National University, South Korea, in 1989 and 1993, respectively, and the Ph.D. degree in mechanical engineering from Tohoku University, Japan. He is currently a Professor with Kunsan National University, South Korea. His research interests include the path planning of robots, artificial intelligence, and the control and measurement of autonomous vehicles.

ZIANG LYU received the M.Eng. degree in mechanical engineering from Kunsan National University, South Korea, in 2023, where he is currently pursuing the Ph.D. degree. His research interests include artificial intelligence, machine learning, and autonomous driving.

HAN ZHANG was born in Xi'an, Shanxi, China. He received the B.S. degree in mechanical design, manufacturing and automatization from the Xi'an University of Science and Technology and the master's degree in mechanical engineering from Xi'an Technological University. He is currently pursuing the Ph.D. degree with Kunsan National University, South Korea. His research interests include machine vision, equipment health status monitoring, and artificial intelligence.